Carrier Landing Robust Control Based on Longitudinal Decoupling

Wu Wenhai, *Wang Jie**, *Liu Jintao*, *Zhang Yuanyuan*, *An Gaofeng*

Naval Aviation University, Qingdao 266041, P. R. China

(Received 25 December 2016; revised 13 July 2017; accepted 20 July 2017)

Abstract: We studied carrier landing robust control based on longitudinal decoupling. Firstly, due to the relative strong coupling between the tangential and the normal directions, the height and the velocity channels were decoupled by using the exact linearization method, so that controllers for the two channels could be designed seperately. In the height control, recursive dynamic surface was used to accelerate the convergence of the height control and eliminate "the explosion of complexity". The RBF neural network was designed by using the minimum learning parameter method to compensate the uncertainty. A kind of surface with nonsingular fast terminal sliding mode and its reaching law were developed to ensure finite time convergence and to avoid singularity. The controller for the velocity was designed by using super-twisting second-order sliding mode control. The stability of the proposed system was validated by Lyapunov method. The results showed that the Levant's robust differential observer was improved and used for the observation of the required higher order differential of signals in the controller. The response of aircraft carrier landing under the complex disturbance is simulated and the results verified the approach.

Key words: carrier landing; recursive dynamic surface; second-order sliding mode; nonsingular fast terminal sliding mode

CLC number: V249.1 **Document code**: A **Article ID**: 1005-1120(2017)06-0609-08

0 Introduction

Carrier landing is the most difficult and dangerous aircraft flight phase of all. Aircraft work in high angle of attack(AOA) and low speed during carrier landing, which is difficult to manipulate and usually disturbed by air wake and their own dynamic perturbation. This phase requires some very high conditions, like response capability, robust performance, and touchdown accuracy. Therefore, many methods have been proposed for carrier landing control law. Subrahmanyam[1] and Yu[2] designed F/A-18A automatic carrier landing system using H-infinity control, and obtained small error of track. The model reference was combined with other methods for automatic landing[3-4]. Intelligent control approaches were also applied to landing control, like fuzzy logic and neural network method[5], adaptive fuzzy neural network method[6], and direct adaptive neural method[7]. Zhu adopted nonlinear dynamic inversion and sliding mode control to design longitudinal carrier landing system[8]. The sliding mode control could provide landing control system strongly robustness for disturbance[9-10]. Yang[11] proposed a robust fault-tolerant control scheme considering input saturation. Fang[12] designed fault tolerant automatic landing controller which presented robustness against disturbances and reliable against actuator stuck faults. Zhen[13] summarized the research on the development of carrier landing guidance and control.

We were to design a robust carrier landing controller, considering the external disturbance, the nonlinear dynamics uncertainty and the coupling in carrier landing. The tangential direction and normal direction (or height and velocity channels) have relatively strong coupling, because ① landing flight is in the backside area of the drag-velocity curve, causing the tangential and normal direction to affect each other; and ② the thrust affects not only the velocity, but also flight path angle in carrier landing because of high angle of

* Corresponding author, E-mail address: reality_123@126.com.

How to cite this article: Wu Wenhai, Wang Jie, Liu Jintao, et al. Carrier landing robust control based on longitudinal decoupling[J]. Trans. Nanjing Univ. Aero. Astro., 2017, 34(6): 609-616.
http://dx.doi.org/10.16356/j.1005-1120.2017.06.609

attack. Therefore, the longitudinal dynamics was decoupled by using the exact linearization method, so that controllers for the height and the velocity channels could be designed seperately.

The design of the height controller involved the method of recursive dynamic surface control in which the recursive design could speed up height error convergence and the dynamic surface control (DSC) technique could eliminate the "explosion of complexity". The radial basis function (RBF) neural network was used to estimate the combined interference, and the minimum learning parameter method was employed to rapidly adjust parameters because of its transformation from multi-parameter adjustment into one-parameter adjustment[14]. A non-singular fast terminal sliding mode surface and a nonsingular fast terminal sliding mode reaching law were designed at last.

The design of velocity controller employed the second-order sliding mode control, not only to ensure the need for robust control, but also to greatly reduce the control surface's chattering, so that the velocity of the landing can be held in trim value in landing.

Differential observer is necessary for estimating the various order derivatives of the height and the velocity signals to implement controller, so the Levant's robust differential observer was used to observe those. The homogeneous terms were added to the original structure to improve the Levant's robust differential observer, for speeding up its dynamics.

1 Model Decoupling

The longitudinal dynamics of carrier-based aircraft landing is as follows

$$\begin{cases} \dot{V}=\dfrac{T\cos(\alpha+\theta_T)-D}{m}-g\sin\gamma \\ \dot{\gamma}=\dfrac{L+T\sin(\alpha+\theta_T)}{mV}-\dfrac{g}{V}\cos\gamma \\ \dot{\alpha}=q-\dot{\gamma},\dot{h}=V\sin\gamma \\ \dot{q}=\dfrac{1}{I_{yy}}(M_a-Tl_T) \\ \ddot{\beta}=-2\xi\omega_n\dot{\beta}-\omega_n^2\beta+\omega_n^2\beta_c \\ T=K_T\beta \end{cases} \tag{1}$$

where h is the height, V the velocity , γ the flight path angle, α the angle of attack, q the pitch angle rate, θ_T the engine installation angle, M_a the aerodynamic moment, β the throttle lever displacement, β_c the throttle lever displacement command, and m and I_{yy} are the mass and the rotation inertia of aircraft, respectively.

The relative rank of the longitudinal dynamics in Eq. (1) is 7. And the input variables can be obtained by calculating the fourth derivative of the height, and the third derivative of the velocity, so the total order of the derivatives is 7. Therefore, the system's relative rank is equal to the total order of derivatives, and the exact linearization can be used for Eq. (1)[15].

The influence of altitude and pitch rate on aerodynamics is very small in landing case, thus their partial derivatives in the Jacobian matrix are very small, and can be ignored. Define vector $\boldsymbol{X}=[V,\gamma,\alpha,\beta]^{\mathrm{T}}$.

The third-order derivative of velocity is calculated as

$$\begin{cases} \dot{V}=\dfrac{T\cos(\alpha+\theta_T)-D}{m}-g\sin\gamma=f_1(\boldsymbol{X}) \\ \ddot{V}=\boldsymbol{\omega}_1\dot{\boldsymbol{X}}/m \\ \dddot{V}=(\boldsymbol{\omega}_2\ddot{\boldsymbol{X}}+\dot{\boldsymbol{X}}^{\mathrm{T}}\boldsymbol{\omega}_1\dot{\boldsymbol{X}})/m \end{cases} \tag{2}$$

The fourth-order derivative of height is

$$\begin{cases} \ddot{h}=V\dot{\gamma}\cos\gamma+\dot{V} \\ h^{(4)}=\dddot{V}\sin\gamma+3\ddot{V}\dot{\gamma}\cos\gamma+3\dot{V}\ddot{\gamma}\cos\gamma- \\ \quad 3\dot{V}\dot{\gamma}^2\sin\gamma-3V\dot{\gamma}\ddot{\gamma}\sin\gamma-V\dot{\gamma}^3\cos\gamma+ \\ \quad V\dddot{\gamma}\cos\gamma \end{cases} \tag{3}$$

where

$$\begin{cases} \dot{\gamma}=\dfrac{L+T\sin(\alpha+\theta_T)}{mV}-\dfrac{g}{V}\cos\gamma=f_2(\boldsymbol{X}) \\ \ddot{\gamma}=\boldsymbol{\omega}_3\dot{\boldsymbol{X}} \\ \dddot{\gamma}=\boldsymbol{\omega}_3\ddot{\boldsymbol{X}}+\dot{\boldsymbol{X}}^{\mathrm{T}}\boldsymbol{\omega}_4\dot{\boldsymbol{X}} \end{cases} \tag{4}$$

where $\boldsymbol{\omega}_1=m\dfrac{\partial f_1}{\partial \boldsymbol{X}},\boldsymbol{\omega}_2=\dfrac{\partial \boldsymbol{\omega}_1}{\partial \boldsymbol{X}},\boldsymbol{\omega}_3=\dfrac{\partial f_2}{\partial \boldsymbol{X}},\boldsymbol{\omega}_4=\dfrac{\partial \boldsymbol{\omega}_3}{\partial \boldsymbol{X}}$.

So we can obtain

$$\begin{bmatrix} \dddot{V} \\ h^{(4)} \end{bmatrix}=\begin{bmatrix} f_V \\ f_H \end{bmatrix}+\begin{bmatrix} g_{11} & g_{12} \\ g_{21} & g_{22} \end{bmatrix}\begin{bmatrix} \beta_c \\ \delta_e \end{bmatrix} \tag{5}$$

where

$$g_{11}=\frac{\rho V^2 S c_{\beta}\omega_n^2}{2m}\cos\alpha$$

$$g_{12}=-\frac{c_e\rho V^2 S\bar{c}}{2mI_y}(T\sin\alpha+\frac{\partial D}{\partial\alpha})$$

$$g_{21}=(\frac{\rho V^2 Sc_\beta\omega_n^2}{2m})\sin(\alpha+\gamma)$$

$$g_{22}=(\frac{c_e\rho V^2 S\bar{c}}{2mI_y})[T\cos(\alpha+\gamma)+\frac{\partial L}{\partial\alpha}\cos\gamma-\frac{\partial D}{\partial\alpha}\sin\gamma]$$

$$f_h=3\ddot{V}\dot{\gamma}\cos\gamma+3\dot{V}\ddot{\gamma}\cos\gamma-3\dot{V}\dot{\gamma}^2\sin\gamma-$$
$$3V\gamma\ddot{\gamma}\sin\gamma-V\dot{\gamma}^3\cos\gamma+$$
$$\frac{(\omega_1\ddot{X}_0+\dot{\boldsymbol{X}}^{\mathrm{T}}\omega_2\dot{\boldsymbol{X}})\sin\gamma}{m}+V\cos\gamma(\omega_3\ddot{\boldsymbol{X}}_0+\dot{\boldsymbol{X}}^{\mathrm{T}}\omega_4\dot{\boldsymbol{X}})$$

$$f_V=(\omega_1\ddot{\boldsymbol{X}}_0+\dot{\boldsymbol{X}}^{\mathrm{T}}\omega_2\dot{\boldsymbol{X}})/m$$

Eq. (5) can be transformed into a triangular standard type as shown in Eqs. (6), (7), where the complex disturbance caused by model perturbation and input disturbance is taken into account

$$\begin{cases}\dot{x}_{V1}=x_{V2}+\Delta x_{V1}\\ \dot{x}_{V2}=x_{V3}+\Delta x_{V2}\\ \dot{x}_{V3}=f_V+u_1+\Delta x_{V3}\\ u_1=g_{11}\beta_c+g_{12}\delta_e\end{cases}\tag{6}$$

$$\begin{cases}\dot{x}_{hi}=x_{h(i+1)}+\Delta x_{hi}\quad i=1,2,3\\ \dot{x}_{h4}=f_h+u_2+\Delta x_{h4}\\ u_2=g_{21}\beta_c+g_{22}\delta_e\end{cases}\tag{7}$$

The RBF neural network is used to estimate the uncertainties. The algorithm is as

$$\xi_j(x)=\exp(-\frac{\|x-c_j\|^2}{2b_j^2})\quad j=1,\cdots,m$$

Take $f(\boldsymbol{X})$ for example, suppose

$$f(\boldsymbol{X})=\boldsymbol{W}^{\mathrm{T}}\xi(x)+\varepsilon$$

where ε is approximation error.

The RBF neural network's output is

$$\hat{f}(\boldsymbol{X})=\hat{\boldsymbol{W}}^{\mathrm{T}}h(x)$$

And define $\tilde{\boldsymbol{W}}=\hat{\boldsymbol{W}}-\boldsymbol{W}$.

In order to accelerate the adjust of neural network for real-time control, so the minimum learning parameter method can be adopted, which the adjustment of the weight vector W can be convert into the adjustment of the weight vector's 2-norm square $\varphi=\|W\|^2$ [14].

2 Height Control Design

The controller for the height is based on Eq. (7).

Step 1 Define the dynamic surface variable $e_{h1}=x_{h1}-x_{h1d}$, where x_{h1d} is the height command signal. And define $e_{hi}=x_{hi}-x_{hid}$; $i=1,2,3$. Define the dynamic surface $s_1=e_{h1}$. The first-order derivative of s_1 is

$$\dot{s}_1=x_{h2}+\Delta x_{h1}-\dot{x}_{h1d},\ \Delta x_{h1}=\boldsymbol{W}_{h1}^{\mathrm{T}}\boldsymbol{\xi}_{h1}+\varepsilon_{h1}\tag{8}$$

Virtual control variable is designed as

$$\bar{x}_{h2}=-\frac{1}{2}s_1\hat{\boldsymbol{\varphi}}_{h1}\boldsymbol{\xi}_{h1}^{\mathrm{T}}\boldsymbol{\xi}_{h1}-k_1s_1-\frac{a_1^2s_1}{2\eta_1}+\dot{x}_{h1d}$$
$$|\varepsilon_{h1}|\leqslant a_1\tag{9}$$

In order to avoid the "explosion of complexity" caused by repeated derivation of $\bar{x}_{h2}$, the first-order low-pass filter is used

$$\tau_2\dot{x}_{h2d}+x_{h2d}=\bar{x}_{h2},\quad x_{h2d}(0)=\bar{x}_{h2}(0)\tag{10}$$

The filtering error

$$y_2=x_{h2d}-\bar{x}_{h2}\tag{11}$$

Substituting Eqs. (9), (11) into Eq. (8), we can obtain

$$\dot{s}_1=e_{h2}+y_{h2}-0.5s_1\hat{\varphi}_{h1}\boldsymbol{\xi}_{h1}^{\mathrm{T}}\boldsymbol{\xi}_{h1}-k_1s_1-$$
$$0.5a_1^2s_1/\eta_1+\boldsymbol{W}_{h1}^{\mathrm{T}}\boldsymbol{\xi}_{h1}+\varepsilon_{h1}\tag{12}$$

Step 2 In order to further reduce the error, the recursive sliding mode method is used to define the dynamic surface[16]

$$s_2=c_1s_1+e_{h2},\ e_{h2}=x_{h2}-x_{h2d}$$
$$\dot{s}_2=c_1\dot{s}_1+(\Delta\dot{s}_2+\Delta x_{h2})+x_{h3}-\dot{x}_{h2d}$$
$$\dot{s}_1=x_{h2}+\hat{\boldsymbol{W}}_{h1}^{\mathrm{T}}\boldsymbol{\xi}_{h1}-\dot{x}_{h1d}$$
$$\Delta s_2=c_1(\dot{s}_1-\dot{\bar{s}}_1)\tag{13}$$

Virtual control variable

$$\bar{x}_{h3}=-c_1\dot{s}_1-\frac{1}{2}s_2\hat{\varphi}_{h2}\boldsymbol{\xi}_{h2}^{\mathrm{T}}\boldsymbol{\xi}_{h2}-k_2s_2-\frac{a_2^2s_2}{2\eta_2}+\dot{x}_{h2d}$$
$$|\varepsilon_{h2}|\leqslant a_2\tag{14}$$

The first-order low pass filter is adopted

$$\tau_3x_{h3d}^2+x_{h3d}=\bar{x}_{h3},x_{h3d}(0)=\bar{x}_{h3}(0)\tag{15}$$

The filtering error

$$y_3=x_{h3d}-\bar{x}_{h3}\tag{16}$$

Step 3 Define recursive sliding surface

$$e_3=x_{h3}-x_{h3d},s_3=c_2s_2+e_3$$

The virtual control variable is obtained

$$\bar{x}_{h4}=-c_2\dot{s}_2-\frac{1}{2}s_3\hat{\varphi}_{h3}\boldsymbol{\xi}_{h3}^{\mathrm{T}}\boldsymbol{\xi}_{h3}-k_3s_3-\frac{a_3^2s_3}{2\eta_3}+\dot{x}_{h3d}\tag{17}$$

The first-order low pass filter is adopted

$$\tau_4\dot{x}_{h4d}+x_{h4d}=\bar{x}_{h4},x_{h4d}(0)=\bar{x}_{h4}(0)\tag{18}$$

An adaptive law is given as follows

$$\dot{\hat{\varphi}}_k=\frac{\lambda_k}{2}s_k^2\boldsymbol{\xi}_{hk}^{\mathrm{T}}\boldsymbol{\xi}_{hk}-\kappa_k\lambda_k\hat{\varphi}_k$$
$$\kappa_k>0,k=1,2,3\tag{19}$$

Define a Lyapunov function as

$$V_{h123}=\sum_{i=1}^{3}\frac{s_i^2}{2}+\sum_{j=2}^{4}\frac{y_{hi}^2}{2}+\sum_{k=1}^{3}\frac{\tilde{\varphi}_{hk}^2}{2\lambda_k}\quad\lambda_k>0\tag{20}$$

Theorem 1 For the above closed-loop subsystem of step 1, 2 and 3, if $V_{h123} \leqslant 2\chi$ and $e_4 = 0$, all the signals are semi-globally uniformly bounded, errors are convergent, the signals the errors can be arbitrarily small by adjusting the parameters of the controller.

Proof From Eqs. (10), (11), (15), (16), we can get

$$\dot{y}_i = \frac{-y_i}{\tau_i} - \dot{\bar{x}}_{hi} = \frac{-y_i}{\tau_i} - B_i \quad i = 2,3,4 \tag{21}$$

Define sets

$$\Omega_1 = \{x_{h1d}^2 + \dot{x}_{h2d}^2 + \ddot{x}_{h3d}^2 \leqslant \nu\} \quad , \Omega_2 = \{V_{123} \leqslant 2\chi\}$$

Then, B_i is bounded. Set $|B_i| \leqslant M_i$.

From the Young's inequality, we can get

$$\frac{a_i^2 s_1^2}{2\eta_i} + \frac{\eta_i}{2} \geqslant a_i |s_i|$$

$$s_1^2 \varphi_{h1} \boldsymbol{\xi}_{h1}^{\mathrm{T}} \boldsymbol{\xi}_{h1} + 1 = s_i^2 \| \boldsymbol{W}_{hi} \|^2 \| \boldsymbol{\xi}_{hi} \|^2 + 1 = s_i^2 \| \boldsymbol{W}_{hi}^{\mathrm{T}} \boldsymbol{\xi}_{hi} \|^2 + 1 \geqslant 2 s_i \boldsymbol{W}_{hi}^{\mathrm{T}} \boldsymbol{\xi}_{hi}$$

$$i = 1,2,3 \tag{22}$$

From Eqs. (12), (22), we can calculate

$$s_1 \dot{s}_1 \leqslant s_1 (e_{h2} + y_{h2} - \frac{1}{2} s_1 \varphi_{h1} \boldsymbol{\xi}_{h1}^{\mathrm{T}} \boldsymbol{\xi}_{h1} - k_1 s_1 - \frac{a_1^2 s_1}{2\eta_1} + \boldsymbol{W}_{h1}^{\mathrm{T}} \boldsymbol{\xi}_{h1} + \varepsilon_{h1}) \leqslant s_1 e_{h2} + s_1 y_{h2} - \frac{1}{2} s_1^2 \hat{\varphi}_{h1} \boldsymbol{\xi}_{h1}^{\mathrm{T}} \boldsymbol{\xi}_{h1} - k_1 s_1^2 - a_1 |s_1| + \frac{\eta_1}{2} + \frac{1}{2} s_1^2 \varphi_{h1} \boldsymbol{\xi}_{h1}^{\mathrm{T}} \boldsymbol{\xi}_{h1} + \frac{1}{2} + \varepsilon_{h1} s_1 \leqslant s_1 e_{h2} + s_1 y_{h2} - \frac{1}{2} s_1^2 \tilde{\varphi}_{h1} \boldsymbol{\xi}_{h1}^{\mathrm{T}} \boldsymbol{\xi}_{h1} - k_1 s_1^2 + \frac{1 + \eta_1}{2}$$

Similarly, we can obtain

$$s_i \dot{s}_i \leqslant s_i e_{h(i+1)} + s_i y_{h(i+1)} - \frac{1}{2} s_i^2 \tilde{\varphi}_{hi} \boldsymbol{\xi}_{hi}^{\mathrm{T}} \boldsymbol{\xi}_{hi} - k_i s_i^2 + \frac{1 + \eta_i}{2}$$

$$i = 2,3 \tag{23}$$

$$\dot{V}_{h123} = \sum_{i=1}^{3} s_i \dot{s}_i + \sum_{j=2}^{4} y_{hj} \dot{y}_{hj} + \sum_{k=1}^{3} \frac{1}{\lambda} \tilde{\varphi}_{hk} \dot{\hat{\varphi}}_{hk} \leqslant \Big(\sum_{i=1}^{2} s_i (s_{(i+1)} - c_i s_i) \Big) + s_3 e_4 + \Big(\sum_{i=1}^{3} s_i y_{h(i+1)} \Big) + \Big(\sum_{i=1}^{3} k_i s_i^2 \Big) + \frac{3}{2} + \sum_{i=1}^{3} \frac{\eta_i}{2} + \sum_{j=2}^{4} y_{hj} (-\frac{y_{hj}}{\tau_j} + B_j) + \Big(-\sum_{i=1}^{3} \frac{1}{2} s_i^2 \tilde{\varphi}_{hi} \boldsymbol{\xi}_{hi}^{\mathrm{T}} \boldsymbol{\xi}_{hi} + \sum_{k=1}^{3} \frac{1}{\lambda_k} \tilde{\varphi}_{hk} \dot{\hat{\varphi}}_{hk} \Big) \leqslant \Big[\sum_{i=1}^{2} (\frac{1}{2} - c_i) s_i^2 + \frac{1}{2} s_{i+1}^2 \Big] + \frac{s_3^2}{2} + \sum_{i=1}^{3} \frac{1}{2} (s_i^2 + y_{h(i+1)}^2) + \Big(\sum_{i=1}^{3} k_i s_i^2 \Big) + \sum_{j=2}^{4} \Big(-\frac{y_{hj}^2}{\tau_j} + \frac{y_{hj}^2}{2} + \frac{B_j^2}{2} \Big) + \frac{3}{2} + \sum_{i=1}^{3} \frac{\eta_i}{2} - \sum_{k=1}^{3} \kappa_k \tilde{\varphi}_{hk} \hat{\varphi}_{hk}$$

Since

$$-\sum_{k=1}^{3} \kappa_k \tilde{\varphi}_{hk} \hat{\varphi}_{hk} \leqslant -\sum_{k=1}^{3} \frac{\kappa_k}{2} (\tilde{\varphi}_{hk}^2 - \varphi_{hk}^2)$$

we can get

$$\dot{V}_{h123} \leqslant (1 - c_1 + k_1) s_1^2 + \Big(\frac{3}{2} - c_2 + k_2 \Big) s_2^2 + \Big(\frac{3}{2} + k_3 \Big) s_3^2 + \sum_{j=1}^{3} \Big(1 - \frac{1}{\tau_j} \Big) y_{hj}^2 - \sum_{k=1}^{3} \frac{\kappa_k}{2} \tilde{\varphi}_{hk}^2 + \frac{3}{2} + \sum_{i=1}^{3} \frac{\eta_i}{2} + \sum_{j=2}^{4} \frac{B_j^2}{2} + \sum_{k=1}^{3} \frac{\kappa_k}{2} \varphi_{hk}^2 \leqslant -(c_1 - 1 - k_1) s_1^2 - \Big(c_2 - \frac{3}{2} - k_2 \Big) s_2^2 - \Big(-\frac{3}{2} - k_3 \Big) s_3^2 - \sum_{j=1}^{3} \Big(\frac{1}{\tau_j} - 1 \Big) y_{hj}^2 - \sum_{k=1}^{3} \frac{\kappa_k}{2} \tilde{\varphi}_{hk}^2 + \frac{3}{2} + \sum_{i=1}^{3} \frac{\eta_i}{2} + \sum_{j=2}^{4} \frac{B_j^2}{2} + \sum_{k=1}^{3} \frac{\kappa_k}{2} \varphi_{hk}^2$$

When taking

$$\kappa_k = \frac{2\mu}{\lambda_k} \quad k = 1,2,3$$

$$Q = \sum_{i=1}^{3} \frac{\eta_i}{2} + \sum_{j=2}^{4} \frac{B_j^2}{2} + \sum_{k=1}^{3} \frac{\kappa_k}{2} \varphi_{hk}^2 + \frac{3}{2}$$

$$\mu = \min \left\{ \begin{matrix} c_1 - 1 - k_1, c_2 - \frac{3}{2} - k_2 \\ c_3 - 1 - k_3, \frac{1}{\tau_i} - 1 \end{matrix} \right\} \quad i = 1,2,3 \tag{24}$$

We can get

$$\dot{V}_{h123} \leqslant -2\mu V_{h123} + Q \tag{25}$$

And when it is taken that $\mu \geqslant Q/2\chi$, and $\dot{V}_{h123} \leqslant 0$, subsystem of steps 1, 2 and 3 is stable and convergent. And if $V_{h123}(0) \leqslant \chi$, we can get $V_{h123}(t) \leqslant \chi$. From Eqs. (25)

$$V_{h123} \leqslant \frac{Q}{2\mu} + (V_{h123}(0) - \frac{Q}{2\mu}) \mathrm{e}^{-2\mu t}$$

Therefore, all signals are bounded. And when $t \to \infty$, it can be gotten that $V_{h123} \to Q/2\mu$. By adjusting the parameters, V_{h123} can be convergent to any small positive number.

Step 4 Define a recursive sliding surface:

$$e_4 = x_{h4} - x_{h4d}, s_4 = e_4$$

The traditional sliding mode surface can only make error gradually convergent to zero. So a kind of nonsingular terminal sliding mode surface is designed to lead error converge to zero in finite time and to avoid the singularity.

Define a kind of non-singular terminal sliding mode where the term σ^l is added to the structure of the ordinary nonsingular terminal sliding mode surface

$$s_4 = \sigma + \beta_1 \sigma^l + \beta_2 \dot{\sigma}^m \quad 1 < l < 2; m > l$$
$$\sigma = \int_0^t e_4(\tau)\mathrm{d}t \tag{26}$$

Remark: Since the differential equation

$$\sigma + \beta_1 \sigma^l + \beta_2 \dot{\sigma}^m = 0 \quad 1 < l < 2; m > l$$

is convergent, Eqs. (26) can be used as a sliding mode surface

$$\dot{s}_4 = e_4 + \beta_1 l \sigma^{l-1} e_4 + \beta_2 m e_4^{m-1} \dot{e}_4 = e_4 + \beta_1 l \sigma^{l-1} e_4 + \beta_2 m e_4^{m-1}(\Delta x_{h4} + f_h + u_2 - \dot{x}_{h4d})$$

The height controller also includes a kind of sliding surface reaching law, as follows

$$u_2 = \frac{-1}{\beta_2 m e_4^{m-1}}[e_4 + \beta_1 m \sigma^{m-1} e_4 + (\beta_3 s_4 + \beta_4 s_4^r)^{\frac{1}{p}}] - \hat{\boldsymbol{W}}_{h4}^{\mathrm{T}} \boldsymbol{\xi}_{h4} - f_h + \dot{x}_{h4d} - a_4 \mathrm{sgn}(s_4)$$
$$|\varepsilon_4| \leqslant a_4; 1 < r < 2; p > r; \beta_i > 0; \quad i = 1,2,3,4 \tag{27}$$

Taking an adaptive law

$$\dot{\hat{\boldsymbol{W}}}_{h4} = \lambda_4 \beta_2 m s_4 e_4^{m-1} \boldsymbol{\xi}_{h4} \tag{28}$$

Proof of stability:

Define a Lyapunov function

$$V_4 = \frac{1}{2} s_4^2 + \frac{1}{2\lambda_4} \boldsymbol{W}_{h4}^{\mathrm{T}} \hat{\boldsymbol{W}}_{h4} \tag{29}$$

$$\dot{V}_4 = s_4 \dot{s}_4 + \frac{1}{\lambda_4} \boldsymbol{W}_{h4}^{\mathrm{T}} \dot{\hat{\boldsymbol{W}}}_{h4} = s_4(-(\beta_3 s_4 + \beta_4 s_4^r)^{\frac{1}{p}}) + s_4 \beta_2 m e_4^{m-1} \cdot (-\tilde{\boldsymbol{W}}^{\mathrm{T}} \boldsymbol{\xi}_{h4} + \varepsilon_4 - a_4 \mathrm{sgn}(s_4)) + \frac{1}{\lambda_4} \boldsymbol{W}_{h4}^{\mathrm{T}} \dot{\hat{\boldsymbol{W}}}_{h4}$$

When taking $m = \rho_1/\rho_2$, $r = \rho_3/\rho_4$, $p = \rho_5/\rho_6$, where ρ_i is odd number, $i = 1, \cdots, 6$, we can get

$$\dot{V}_4 \leqslant s_4(-(\beta_3 s_4 + \beta_4 s_4^r)^{\frac{1}{p}}) \leqslant 0 \tag{30}$$

Then it can be known that the subsystem of step 4 is convergent.

And since $\tilde{\boldsymbol{W}} \to 0, \tilde{\boldsymbol{W}} \to 0$, we can obtain

$$s_4 \dot{s}_4 \leqslant -s_4(\beta_3 s_4 + \beta_4 s_4^r)^{1/p} \leqslant 0$$
$$\dot{s}_4 \leqslant -(\beta_3 s_4 + \beta_4 s_4^r)^{1/p} \leqslant 0 \tag{31}$$

From Eq. (31), it can be seen that the subsystem of step 4 is convergent in finite time.

In conclusion, the subsystem 4 is convergent to $s_4 = 0$ in finite time in the effect of controller in Eqs. (27) and the adaptive law. And according to Theorem 1, the subsystems of steps 1, 2 and 3 converge, all the signals are bounded, and the error can be arbitrarily small by adjusting the parameters. And the saturation function can be used in place of the symbolic function "sgn" in the above controller.

3 Velocity Control Design

The velocity controller is designed based on Eqs. (6).

Define $e_V = V - V_d$.

Since the velocity is instable without control in carrier landing, the super-twisting second-order sliding mode control is applied to the control/hold of the velocity[17-18].

Define a sliding mode surface as follows

$$s_V = \ddot{e}_V + a_2 \dot{e}_V + a_1 e_V$$
$$\dot{s}_V = a_2 \ddot{e}_V + a_1 \dot{e}_V + f_V + u_1 + \Delta x_{V3} + \Delta \dot{x}_{V2} + \Delta \ddot{x}_{V1} - \dddot{x}_{v1d}$$

The controller is

$$u_1 = u_{eq} + u_{sw}$$
$$u_{eq} = -a_2 \ddot{e}_V - a_1 \dot{e}_V - f_V + \dddot{V}_d - \hat{\boldsymbol{W}}_V^{\mathrm{T}} \boldsymbol{\xi}_V$$
$$u_{sw} = -\mu |s_V|^{1/2} \mathrm{sgn}(s_V) + z$$
$$\dot{z} = -k \mathrm{sgn}(s_V) \tag{32}$$

Taking an adaptive law as follows

$$\dot{\hat{\boldsymbol{W}}}_{h4} = \lambda_V s_V \boldsymbol{\xi}_V \tag{33}$$

Proof of stability

$$V_V = \frac{1}{2} s_V^2 + \frac{1}{2\lambda_V} \boldsymbol{W}_V^{\mathrm{T}} \boldsymbol{W}_V \tag{34}$$
$$\dot{V}_V \leqslant s_V(-\mu_1 |s_V|^{1/2} \mathrm{sgn}(s_V) + z) \leqslant 0$$
$$\hat{\boldsymbol{W}}_V \to 0 \tag{35}$$

Therefore, we can get

$$\dot{s}_V \leqslant -\mu_1 |s_V|^{1/2} \mathrm{sgn}(s_V) + z \tag{36}$$

According to the comparison principle and conclusions in Refs. [17—18], we know that the sliding mode surface converge is in finite time.

Then we can get the control law of aircraft's throttle and elevator

$$\begin{bmatrix} \beta_c \\ \delta_e \end{bmatrix} = \begin{bmatrix} g_{11} & g_{12} \\ g_{21} & g_{22} \end{bmatrix}^{-1} \begin{bmatrix} u_1 \\ u_2 \end{bmatrix} \tag{37}$$

4 Differential Observer Design

To complete the controller, we need to the necessary order derivatives of the height and the velocity, but they will magnify noise to compute

derivatives directly. However, the Levant′s robust differential observer[18] is able to guarantee the robustness and control precision without magnifying noise. In order to accelerate its dynamics, the Levant′s robust differential observer is improved by adding homogeneous terms $-\bar{\omega}_i e$, as follows

$$\begin{aligned}
&\dot{z}_0 = v_0, v_0 = F_0(z_0 - f(t)) + z_1\\
&\dot{z}_i = v_i, v_i = F_i(z_i - v_{i-1}) + z_{i+1}\\
&\vdots\\
&\dot{z}_n = F_n(z_n - v_{n-1})\\
&F_i(e) = -\omega_i L^{\frac{1}{n+1-i}} |e|^{\frac{n-i}{n+1-i}} \operatorname{sgn}(e) - \bar{\omega}_i e\\
&0 < d_i < 1; i = 1, \cdots, n-1
\end{aligned} \tag{38}$$

Let $f(t)=h(t), n=3$, then the necessary order derivatives of height signal can be obtained using Eq. (38). Let $f(t)=V(t), n=2$, then the necessary order derivatives of velocity signal can be obtained either.

5 Simulation

In order to verify the feasibility of the proposed controllers, the simulation of carrier landing was built. Simulation time was set as 56.3 s. The height initial deviation of 1 m was given at the beginning, and the air wake interference was encountered in the last 12.5 s. The aircraft′s aerodynamic parameters were perturbed by a same proportion of 50%. Δx_{h4} and Δx_{V3} were the sum of the white noise with a power of 0.001, and sine signal with an amplitude of 0.01 and frequency 1 rad/s. $\Delta x_{h1}, \Delta x_{h1}, \Delta x_{h1}, \Delta x_{h1}, \Delta x_{V1}, \Delta x_{V2}$ were all sine signals with an amplitude of 0.001, and a frequency 1 rad/s. Filter′ time constants were all turned to 0.004. The trim states were: V = 69.3 m/s, $\alpha = 8.5°$, $\theta = 5°$, elevator $\delta_e = -3.17°$, throttle β = 43%. The simulation results are shown in Fig. 1.

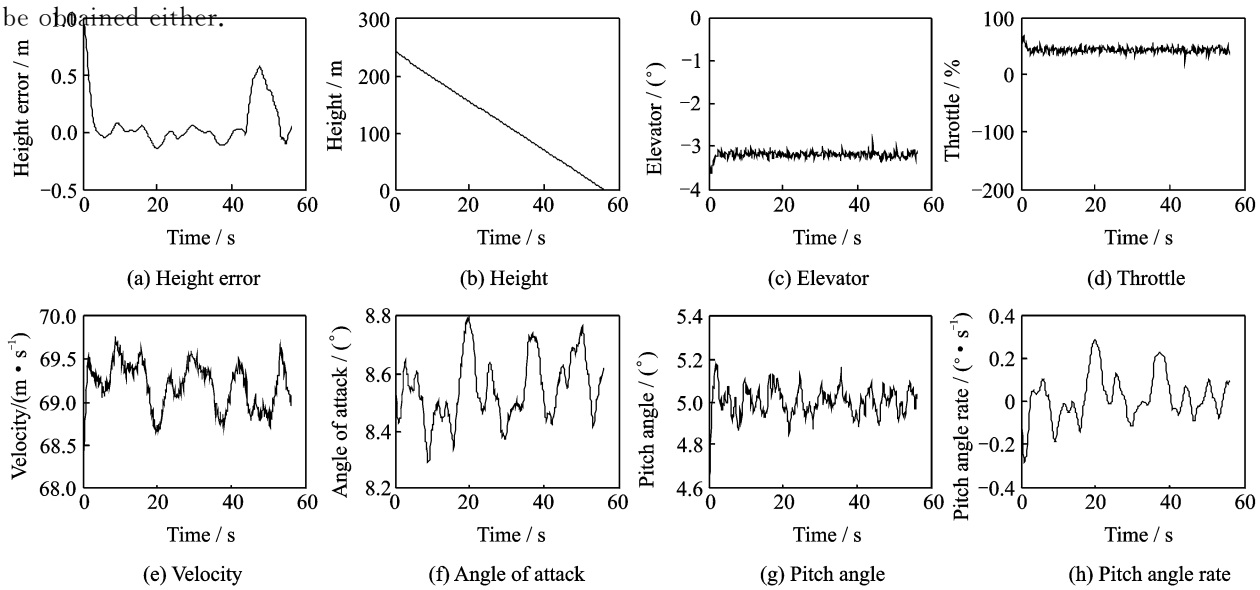

Fig. 1 System response in carrier landing glide phase(with complex disturbance)

When there was an initial 1 m height deviation at the beginning of the simulation, the system responsed quickly to correct the deviation, and the height error was eliminated to zero at time of 3 s. Because of the existence of complex disturbance described above, the height and other states were changing near trim states, in a small bound after the time of 3 s. At the time of 43.8 s, the air wake began to affect aircraft, causing it to firstly fly up and then down. The height error was in bounded 0.6 m in the last 12.5 s, and the height error in the ideal landing point was only within 0.1 m, less than 0.7 m required for the carrier landing criterion. In the whole process, the changes of states (like velocity, AOA and so on), and the changes of control surfaces were all in a small and accepted area. Therefore, it can be considered that the controller can achieve robust performance and guidance precise in carrier landing.

6 Conclusions

The carrier landing robust and the self-adaptive control have been studied, considering inter-

nal uncertainties and external disturbances of the nonlinear dynamics of carrier-based aircraft. Theories and simulations verify the approach. And the following conclusions are obtained.

(1)Theexact linearization method is able to decouple the carrier-based aircraft dynamics model. Robust control method is required to cancel the uncertain factors in the model, so that the effectiveness of the exact linearization can be ensured.

(2) The minimal learning parameter method can obviously improve the ability of estimating the uncertainties of the RBF neural networks, and the problem of "dimensionality curse" is solved.

(3) The combination of recursive dynamic surface and nonsingular fast terminal sliding mode can improve the convergence rate.

(4) Homogeneous items result in better convergence performance of Levant's robust differentiator.

Acknowledgments

This work was supported in part by the National Natural Science Foundation of China (No. 51505491). The authors would like to acknowledge the following people for their assistance: Gao Li, Zhou Siyu, Zhang Yang, Gao Yang, all from the Laboratory of Flight Control, Qingdao Branch, Naval Aeronautical University.

References:

[1] SUBRAHMANYAM M B. H-infinity design of F/A-18A automatic carrier landing system[J]. Journal of Guidance Control & Dynamics, 1994, 17(4): 187-191.

[2] YU Y, YANG Y D, DAI S J. Study of flight/thrust control system using Hinf synthesis in carrier landing system[J]. Journal of Nanjing University of Science and Technology, 2003, 27(3): 256-260. (in Chinese)

[3] JIAO X, JIANG J, WANG X H, et al. Air wake rejecting method based on model reference fuzzy adapting system control [J]. Journal of Nanjing University of Aeronautics & Astronautics, 2013, 45(3): 396-401. (in Chinese)

[4] ZHU Q D, WEN Z X, ZHANG Z, et al. Carrier aircraft landing mixed Hinf/H2 LPV model reference control during powered approach[J]. Journal of Harbin Engineering University, 2013, 34(1): 83-91. (in Chinese).

[5] BOELY N, BOTEZ R M, KOUBA G, Identification of a non-linear F/A-18 model by the use of fuzzy logic and neural network methods [J]. Journal of Aerospace Engineering, 2010, 225(5): 559-574.

[6] JUANG J G, CHIEN L H. Adaptive fuzzy neural network control for automatic landing system [J]. Lecture Notes in Computer Science, 2010, 6421(1): 530-530.

[7] SURESH S, OMKAR S N, MANI V, et al. Direct adaptive neural flight controller for F-8 fighter aircraft [J]. Journal of Guidance, Control and Dynamics, 2006, 29(2): 454-464.

[8] ZHU Q D, MENG X, ZHANG Z, Design of longitudinal carrier landing system using nonlinear dynamic inversion and sliding mode control [J]. Systems Engineering & Electronics, 2014, 36(10): 2037-2042.

[9] JUANG J G, YU S T, Disturbance encountered landing system design based on sliding mode control with evolutionary computation and cerebellar model articulation controller [J]. Applied Mathematical Modelling, 2015, 39(19): 5862-5881.

[10] RAO D M, GO T H, Automatic landing system design using sliding mode control [J]. Aerospace Science & Technology, 2014, 32(1): 180-187.

[11] YANG Q Y, CHEN M. Robust fault-tolerant control for longitudinal dynamics of aircraft with input saturation [J]. Transactions of Nanjing University of Aeronautics and Astronautics, 2016, 33(3): 319-328.

[12] FANG L, JIAN L W, ENG K P. Fault-tolerant robust automatic landing control design [J]. Journal of Guidance Control & Dynamics, 2005, 28(5): 854-871.

[13] ZHEN Z Y, WANG X H, JIANG J, et al. Research development in guidance and control of automatic carrier landing of carrier-based aircraft [J]. Acta Aeronautica et Astronautica Sinica, 2017, 38(2): 122-143. (in Chinese)

[14] BING C, LIU X P, LIU K F. Direct adaptive fuzzy control of nonlinear strict-feedback systems [J]. Automatica, 2009, 45(6): 1530-1535.

[15] WANG Q. Researeh on flight control system desigining theories and simulation for a hypersonic vehicle [D]. Shanghai: Fudan University, 2011: 38-60. (in Chinese)

[16] LIANG S, SUN X X. Nonlinear control based on nonlinear gain of hypersonic vehicle [J]. Flight Dy-

namics, 2015, 33(6): 527-531. (in Chinese)
[17] LEVANT A. Sliding order and sliding accuracy in sliding mode control [J]. International Journal of Control, 1993, 58(6): 1247-1263.
[18] LEVANT A. Higher order sliding modes, differentiation and output-feedback control[J]. International Journal of Control, 2003, 76(9): 924-941.

Prof. **Wu Wenhai** received his B. S. and Ph. D. degrees in automation from Nanjing University of Aeronautics and Astronautics (NUAA), Nanjing, China, in 1983 and 2004, respectively. Since 1983, he has been working at the Qingdao Branch, Naval Aviation University. His research is focused on A/C guidance & control.

Mr. **Wang Jie** received his B. S. degree in electric engineering and automation from Nanchang Aeronautical University in 2011, and M. S. degree in instrument science and technology from Naval Aeronautical and Engineering Institute in 2013. He is studying in Naval Aviation University for Ph. D.

Dr. **Liu Jintao** received his B. S. and Ph. D. degrees in control science and engineering from Naval Aeronautical and Engineering Institute, Beijing, China, in 2003 and 2017, respectively. His research is focused on unmanned systems, navigation and control.

Dr. **Zhang Yuanyuan** received B. S. degree in electric engineering and automation from Air Force Aviation University in 2005 and Ph. D. degree in control science and engineering from Naval Aeronautical and Engineering Institute in 2016, respectively. His research is focused on intelligent decision and process modeling.

Mr. **An Gaofeng** received his B. S. degree in automation from Weifang Institute in 2012, and M. S. degree in control science and engineering from Nanchang Aviation University in 2015. His research is focused on computer program.

(Executive Editor: Zhang Bei)